Heavy Quark Production Measurements at THERA *

15th May 2001

L. Gladilin
Weizmann Institute, Department of Particle Physics,
Rehovot, Israel
on leave from Moscow State University
gladilin@mail.desy.de

I. Redondo
Universidad Autónoma de Madrid,
Departamento de Física Teórica, Madrid, Spain
redondo@mail.desy.de

Abstract

The total cross sections of charm and beauty production at a future high–energy ep collider, THERA, are expected to increase by factors of three and five, respectively, as compared to HERA. Heavy quarks can be measured at THERA in wide ranges of transverse momenta and Q^2 values, thereby providing a solid basis for testing the perturbative QCD calculations. The charm and beauty contributions to the proton structure can be probed at THERA at ~ 1 order of magnitude smaller Bjorken x values with respect to those at HERA. Charm production in the process of photon–gluon fusion at THERA can serve for the determination of the gluon structure of the proton in the as yet unexplored kinematic range $10^{-5} < x_g < 10^{-4}$. The cross section of charm production in charged current at THERA is ~ 1 order of magnitude larger than that at HERA.

*To appear in "The THERA Book", DESY-LC-REV-2001-062 (2001).

1 Introduction

Heavy quarks are produced copiously at HERA which provides collisions between electrons or positrons with energy $E_e = 27.5\,\mathrm{GeV}$ and protons with energy $E_p = 920\,\mathrm{GeV}$ [1]. The total charm and beauty cross sections at HERA are of the order of $1\,\mu\mathrm{b}$ and $10\,\mathrm{nb}$, respectively [?]. In photoproduction processes at HERA, a quasi-real photon with virtuality $Q^2 \sim 0$ is emitted by the incoming electron and interacts with the proton. At leading order (LO) in QCD two types of processes are responsible for the production of heavy quarks: the direct photon processes, where the photon participates as a point-like particle, and the resolved photon processes, where the photon acts as a source of partons. The dominant direct photon process is photon–gluon fusion (PGF) where the photon fuses with a gluon from the incoming proton. In resolved photon processes, a parton from the photon scatters off a parton from the proton. Charm and beauty quarks present in the parton distributions of the photon, as well as of the proton, lead to processes like $cg \to cg$ and $bg \to bg$, which are called heavy flavour excitation processes. In next-to-leading order (NLO) QCD only the sum of direct and resolved processes is unambiguously defined. The resolved photon processes are suppressed in deep inelastic scattering (DIS) at HERA because the virtuality of the exchanged photon is typically selected to be $Q^2 > 1\,\mathrm{GeV}^2$.

Charm production at HERA has been studied by the H1 and ZEUS collaborations in both the photoproduction and DIS regimes [?, ?, ?, ?]. A description of the charm photoproduction cross sections is rather problematic for present perturbative QCD (pQCD) calculations. The fixed-order NLO calculations [?] are generally below the measured cross sections, in particular in the forward (proton) direction [?, ?]. The fixed-order approach assumes that gluons and light quarks (u,d,s) are the only active partons in the structure functions of the proton and the photon. In this approach there is no explicit heavy flavour excitation component and heavy quarks are produced only dynamically in hard pQCD processes. The resummed NLO calculations [?, ?, ?] treat charm as an additional active parton in the structure functions. These calculations are valid only if the heavy quark transverse momentum is much larger than $M_{c,b}$, where $M_{c,b}$ is the charm or beauty quark mass. The resummed NLO predictions of [?, ?] are rather close to the measured cross sections [?].

The fixed-order or three flavour Fixed Flavour Number Scheme (FFNS) calculations for charm production in DIS [?] agree with the cross sections measured at HERA [?, ?]. These calculations are expected to be less reliable when $Q^2/M_c^2 \gg 1$. In this range the $\ln(Q^2/M_c^2)$ terms should be resummed and absorbed into the charm distribution function in the proton [?, ?, ?].

The first measured beauty photoproduction cross sections at HERA [?, ?] lie above the fixed-order NLO QCD predictions [?, ?]. The preliminary value of the beauty production cross section in the DIS regime at HERA, reported recently by the H1 collaboration [?], exceeds the FFNS prediction [?].

Future THERA collider will utilize proton beam from HERA and electron beam prepared with one or both arms of the TESLA e^+e^- linear collider. Using only one arm of the electron accelerator, electron energies of 250 GeV and 400 GeV can be reached in the first and second stages of TESLA, respectively. The electron energy can be as large as 800 GeV employing both TESLA arms. An increase of the centre-of-mass energy of ep

[1] The proton energy was 820 GeV from 1992 to 1997.

collisions from about 300 GeV at HERA to ~ 1 TeV at THERA will result in quite significant increase of the total heavy quark production cross sections. Tables 1 and 2 show LO estimations of the cross sections in direct and resolved photon processes, respectively. The estimations were obtained with the LO Monte Carlo program HERWIG [**?**].

Collider	charm [μb]	beauty [nb]	top [fb]
HERA, $E_e = 27.5\,\text{GeV}$	0.6	4.3	–
THERA, $E_e = 250\,\text{GeV}$	1.6	17	6.9
THERA, $E_e = 400\,\text{GeV}$	1.9	22	26
THERA, $E_e = 800\,\text{GeV}$	2.4	32	$1.2 \cdot 10^2$

Table 1: Cross sections of charm, beauty and top production in direct photon processes at HERA and THERA estimated with the LO Monte Carlo program HERWIG.

Collider	charm [μb]	beauty [nb]	top [fb]
HERA, $E_e = 27.5\,\text{GeV}$	0.3	1.4	–
THERA, $E_e = 250\,\text{GeV}$	1.2	14	0.2
THERA, $E_e = 400\,\text{GeV}$	1.6	21	0.6
THERA, $E_e = 800\,\text{GeV}$	2.5	38	1.9

Table 2: Cross sections of charm, beauty and top production in resolved photon processes at HERA and THERA estimated with the LO Monte Carlo program HERWIG.

The total charm and beauty production cross sections at THERA with $E_e = 250\,\text{GeV}$ are larger than those at HERA by factors ~ 3 and ~ 5, respectively. They grow further with the increase of the electron beam energy. The growth is larger for heavy quark production in the resolved photon processes. The total cross sections of top quark production at THERA with $E_e = 250\,\text{GeV}$ and $E_e = 800\,\text{GeV}$ are of the order of 10 fb and 100 fb, respectively.

2 Heavy quark photoproduction and proton gluon structure

Charm and beauty production in ep collisions is dominated by photoproduction with $Q^2 \sim 0$. In this regime both direct and resolved photon contributions are sizable. Prospects for investigations of heavy quark production in resolved photon processes at THERA are discussed elsewhere in this book [**?**]. In this section we will discuss charm and beauty photoproduction in direct photon processes and its sensitivity to the gluon structure of the proton.

Fig. 1 shows the contributions of photon–gluon fusion to the differential cross sections $d\sigma/dp_\perp^{c,b}$ and $d\sigma/d\eta^{c,b}$ ($p_\perp^{c,b}$ and $\eta^{c,b}$ denoting the quark transverse momentum and pseudorapidity [2]) at HERA and THERA, calculated within NLO QCD [**?**] for $Q^2 < 1\,\text{GeV}^2$. The difference between the heavy quark production cross sections at THERA and HERA increases with increasing $p_\perp^{c,b}$, thereby creating the opportunity to measure charm and

[2]The pseudorapidity η is defined as $-\ln(\tan\frac{\theta}{2})$, where the polar angle θ is taken with respect to the proton beam direction.

beauty quarks at THERA in a wider transverse momentum range. Such measurements will provide a solid basis for testing the fixed-order, resummed, and k_t-factorization [**?**] pQCD calculations. One has to note that the heavy quark pseudorapidity distributions are shifted to backward (electron) direction at THERA with respect to those at HERA. To measure charm and beauty hadronization products a detector for THERA should be equiped with special tracking and muon identification devices in the backward direction.

Measurements of the heavy quarks produced in the process of photon–gluon fusion can be used for the direct reconstruction of the gluon structure of the proton [**?**]. Fig. 2 shows the differential cross sections $d\sigma/d\log_{10} x_g$ (x_g denoting the gluon fractional momentum in the proton) for charm and beauty produced in PGF at HERA and THERA. The cross sections were calculated within NLO QCD [**?**] for $Q^2 < 1\,\mathrm{GeV}^2$. The increase of the electron beam energy will provide an opportunity to probe at THERA one order of magnitude smaller x_g values with respect to those at HERA. The kinematic limits of the x_g measurements at THERA are 10^{-5} and 10^{-4} for charm and beauty production, respectively. However, to be sensitive to the x_g values around the kinematic limits one will need to tag heavy quarks in the very backward direction at THERA. Plots (c) and (d) in Fig. 2 show the predictions for THERA with $E_e = 250\,\mathrm{GeV}$ imposing additional cuts $\theta^{c,b} < 179^\circ$, $\theta^{c,b} < 175^\circ$ and $\theta^{c,b} < 170^\circ$. Only charm quarks with $\theta^c > 175^\circ$ demonstrate sensitivity to the as yet unexplored range $10^{-5} < x_g < 10^{-4}$.

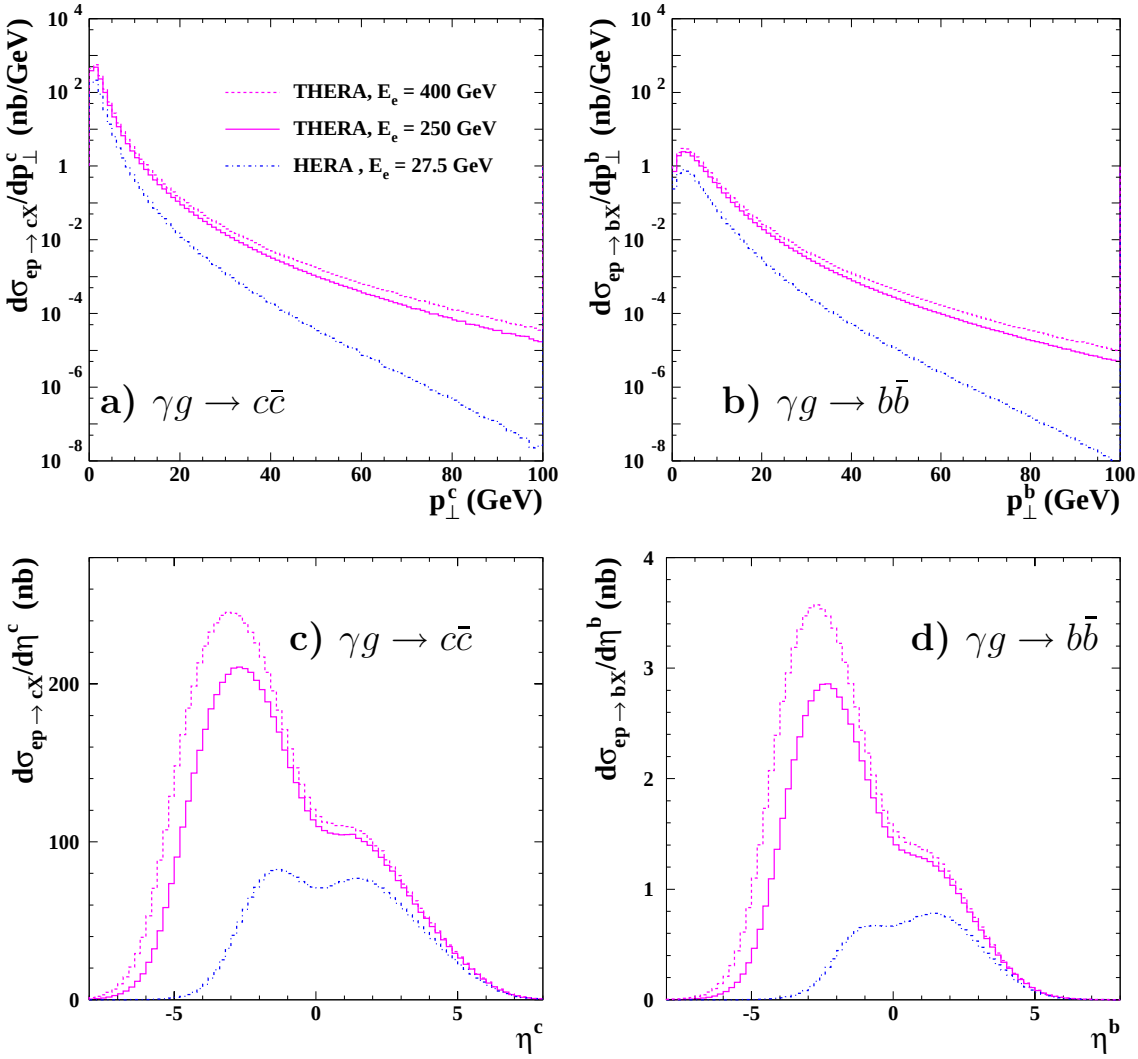

Figure 1: The contribution of photon–gluon fusion to the differential cross sections $d\sigma/dp_\perp$ and $d\sigma/d\eta$ for charm ((a) and (c)) and beauty ((b) and (d)) production calculated in NLO QCD for $Q^2 < 1\,\mathrm{GeV}^2$. The solid and dashed magenta curves show the predictions for THERA operation with an electron energy of 250 GeV and 400 GeV, respectively, and $E_p = 920\,\mathrm{GeV}$. The predictions for the HERA case are indicated by the dash-dotted blue curves.

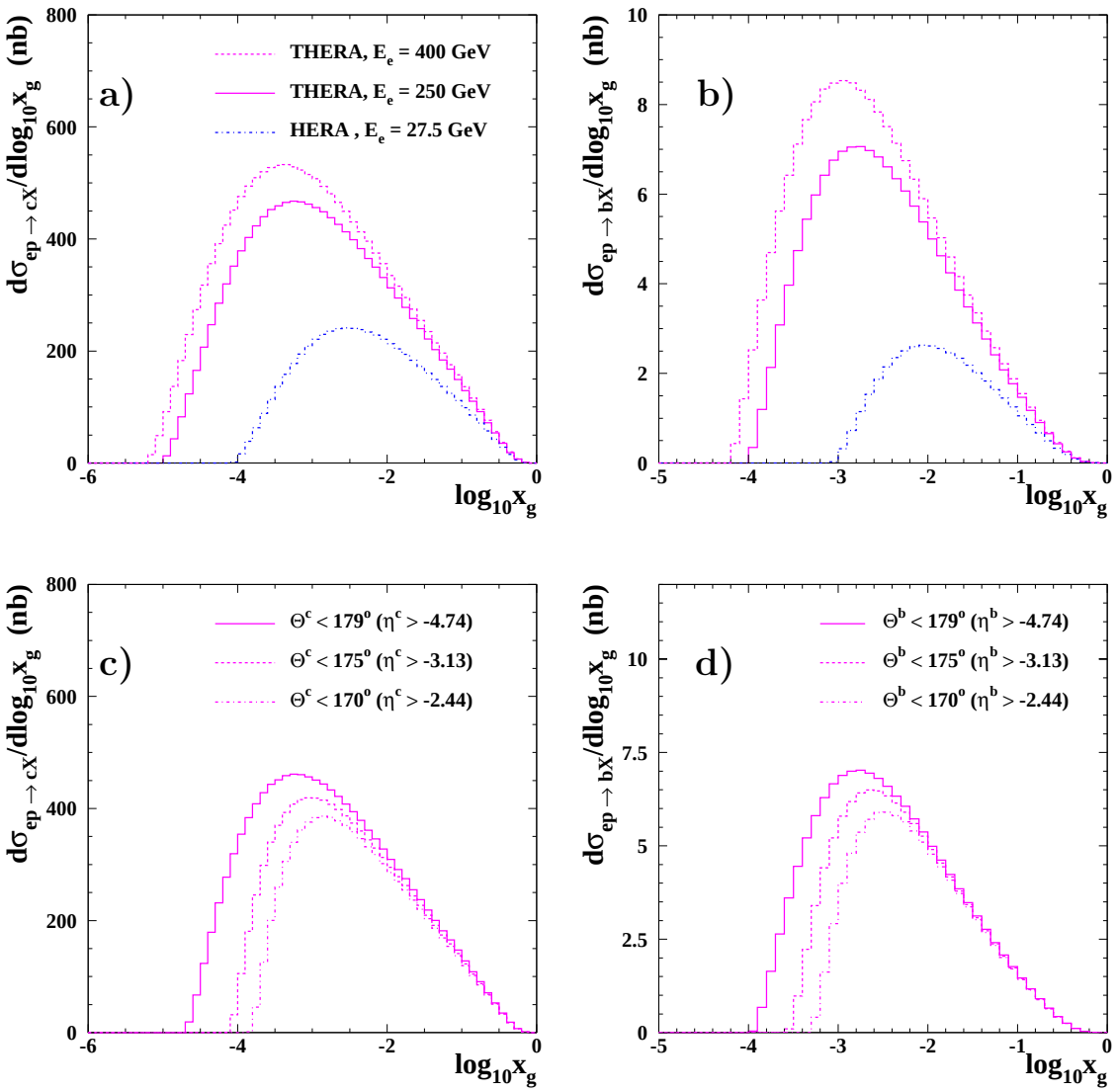

Figure 2: The differential cross sections $d\sigma/d\log_{10} x_g$ for charm ((a) and (c)) and beauty ((b) and (d)) produced in the process of photon–gluon fusion. The cross sections were calculated within NLO QCD for $Q^2 < 1\,\mathrm{GeV}^2$. In (a) and (b), the solid and dashed magenta curves show the predictions for THERA operation with an electron energy of 250 GeV and 400 GeV, respectively, and $E_p = 920\,\mathrm{GeV}$. The predictions for the HERA case are indicated by the dash-dotted blue curves. In (c) and (d), the predictions for THERA with $E_e = 250\,\mathrm{GeV}$ are shown with additional cuts $\theta^{c,b} < 179°$ (solid curves), $\theta^{c,b} < 175°$ (dashed curves) and $\theta^{c,b} < 170°$ (dash-dotted curves).

3 Heavy quark production in neutral current DIS

Electron–proton scattering at $\sqrt{s} \sim 1\,\mathrm{TeV}$ will open new regions for heavy quark production in DIS never measured before. One of the legacies of HERA is the experimental confirmation that charm electroproduction in the HERA regime is dominated by PGF [**?**, **?**]. It is, therefore, a direct probe of the gluon in the proton.

A NLO QCD Monte Carlo program HVQDIS [**?**] was used to study the sensitivity for charm and bottom production at THERA with respect to that at HERA focusing in the increased reach at small Bjorken x values. The HVQDIS program produces fully differential distributions in the heavy quark momenta. It implements three flavour FFNS matrix elements to order α_s^2 calculated previously in [**?**], and gives a fair description of charm electroproduction at HERA [**?**].

It was assumed that scattered electrons will be measurable down to very low angles allowing sizable acceptance for DIS events with $Q^2 > 1\,\mathrm{GeV}^2$. Fig. 3 shows the scattered electron angle and energy constant lines for HERA and THERA. The angle line corresponding to the current ZEUS detector limit (177.5 degrees) excludes most of the region bellow $Q^2 = 100\,\mathrm{GeV}^2$ at THERA. Thus, to measure scattered electrons in the low Q^2 DIS range one will need a special low angle detector at THERA.

Minimum cuts on the $p_\perp$ and η of the heavy quarks were imposed to take into account the detector acceptance for the heavy quark tagging. The choices made here are an educated guess, which can be considered optimistic.

The following kinematic range was selected:

- $Q^2 > 1\,\mathrm{GeV}^2$
- $p_\perp^{c,b} > 3\,\mathrm{GeV}$
- $\mid \eta^{c,b} \mid < 5$

HVQDIS was run with the following settings unless otherwise stated:

- $E_e = 250\,\mathrm{GeV}$ and $E_p = 1\,\mathrm{TeV}$ for THERA
- parton densities in the proton: GRV98 [**?**]
- renormalization scale = factorization scale = $\sqrt{Q^2 + 4M_{c,b}^2}$
- $M_c = 1.4; M_b = 4.5\,\mathrm{GeV}$

Fig. 4 displays the differential cross sections $d\sigma/d\log_{10} Q^2$ and $d\sigma/d\log_{10} x$ for charm and beauty production at THERA and HERA in the kinematic region defined above. The most prominent difference is the increase of the cross sections for both charm and beauty at low x. The cross sections are experimentally measurable at values as low as 10^{-6}. The effect of increasing the energy of the electron beam to 400 GeV is shown in Fig. 6.

Fig. 7 illustrates the extension of the kinematic range of the $F_2^{c\bar{c}}$ measurement from HERA to THERA. $F_2^{c\bar{c}}$ at Q^2 values between 1.8 and $600\,\mathrm{GeV}^2$ is plotted as a function of x. The $F_2^{c\bar{c}}$ values measured by the ZEUS collaboration [**?**] are shown as an illustration. The expected extension is plotted as vertical shaded (yellow) bands. The bands have been produced from the difference of the THERA and HERA low x limits obtained

with HVQDIS. The curves in Fig. 7 correspond to the three flavour FFNS NLO QCD calculation [**?**] using the parton distributions from the ZEUS NLO QCD fit [**?**]. The figure shows a gain of ~ 1 order of magnitude in x for all Q^2 values. And, since $F_2^{c\bar{c}}$ and the gluon density at larger Q^2 values increase steeper towards small x, the gain in the accepted x range produces an increase of the ratio between THERA and HERA cross sections with Q^2. This ratio rises from $\sim$3(3.5) at low Q^2 to $\sim$5(5.5) at $\log_{10}(Q^2)$=3.5 for charm (beauty) production. Of course, to benefit from the rise and to improve substantially HERA results in the high Q^2 region, THERA luminosity should be of the same order as the final HERA luminosity ($\sim 1\,\mathrm{fb}^{-1}$).

The gain in the acceptance to low x values will be marginal if it will be impossible to measure DIS with Q^2 below $10\,\mathrm{GeV}^2$ at THERA. Fig. 3 shows the differential cross sections for charm quark production at THERA (solid curve) and HERA (dashed curve). The effect of the $Q^2 > 10\,\mathrm{GeV}^2$ requirement for the THERA case is shown by the dash-dotted curve. THERA sensitivity to low x values depends also on the η range of the heavy quark tagging. The dotted curve shows the THERA cross section with the cut $\mid \eta^c \mid$<3 used instead of $\mid \eta^c \mid$<5. Relaxing the minimum $p_\perp^c$ cut leads to a gain in the accepted THERA cross section but not in the low x reach.

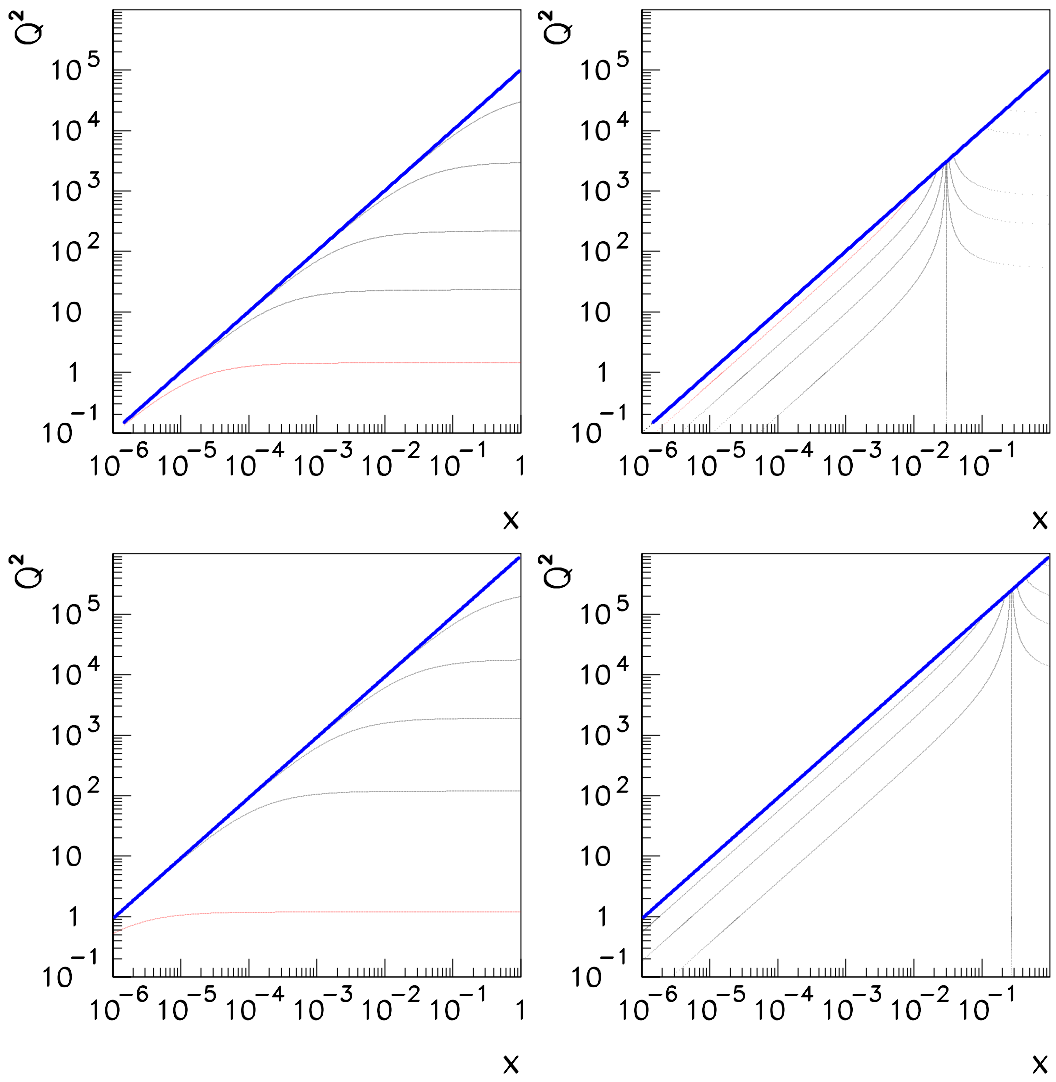

Figure 3: The scattered electron angle (left) and energy (right) constant lines in the Q^2 and x plane. Top (bottom) plots are for HERA (THERA) kinematics. Thick (blue) diagonal lines are the kinematic limits. The values of constant angle and energy lines plotted for HERA(THERA) kinematics are 177.5, 170, 150, 90, 30 (179.75, 177.5, 170, 150, 90) degrees and 10, 20, 25, 27, 27.5, 28, 30, 35, 100, 200 (10, 100, 200, 240, 250, 260, 300, 400, 500) GeV. The 10 GeV line is indistinguishable from the kinematic limit in the case of THERA.

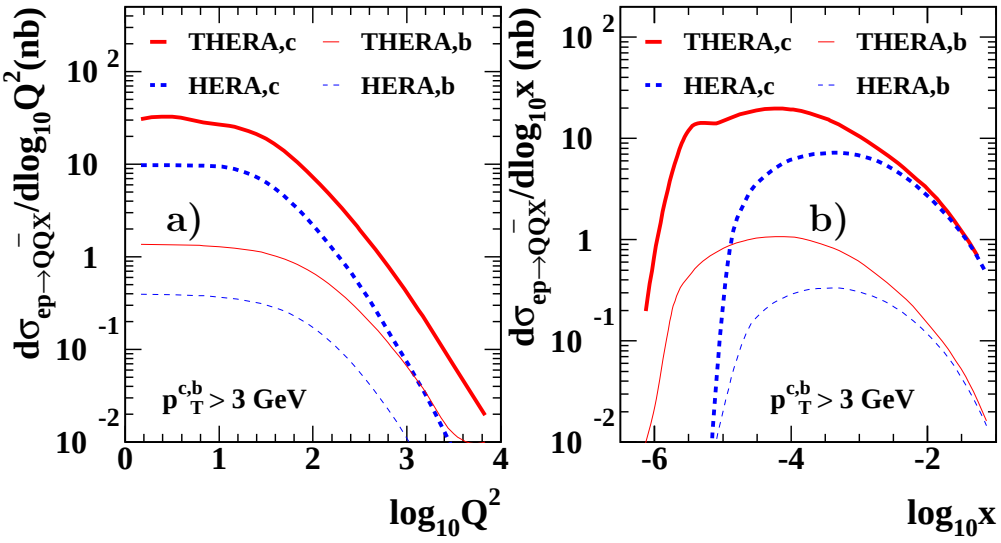

Figure 4: The differential cross sections for charm (thick curves) and beauty (thin curves) production in neutral current DIS calculated in NLO QCD, (a) $d\sigma/d\log_{10}Q^2$ and (b) $d\sigma/d\log_{10}x$. The cross sections at THERA (solid red curves) and HERA (dashed blue curves) are compared.

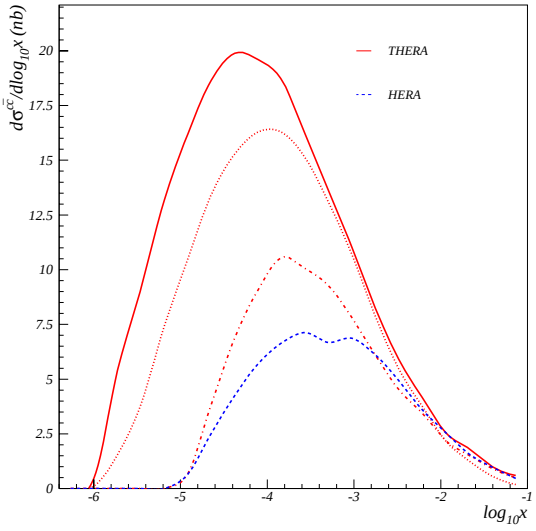

Figure 5: The differential cross sections $d\sigma/d\log_{10}x$ for charm quark production at THERA (solid red curve) and HERA (dashed blue curve). The dash-dotted and dotted red curves show the cross sections for THERA with the additional cuts $Q^2 > 10\,\mathrm{GeV}^2$ and $|\,\eta^c\,|<3$, respectively.

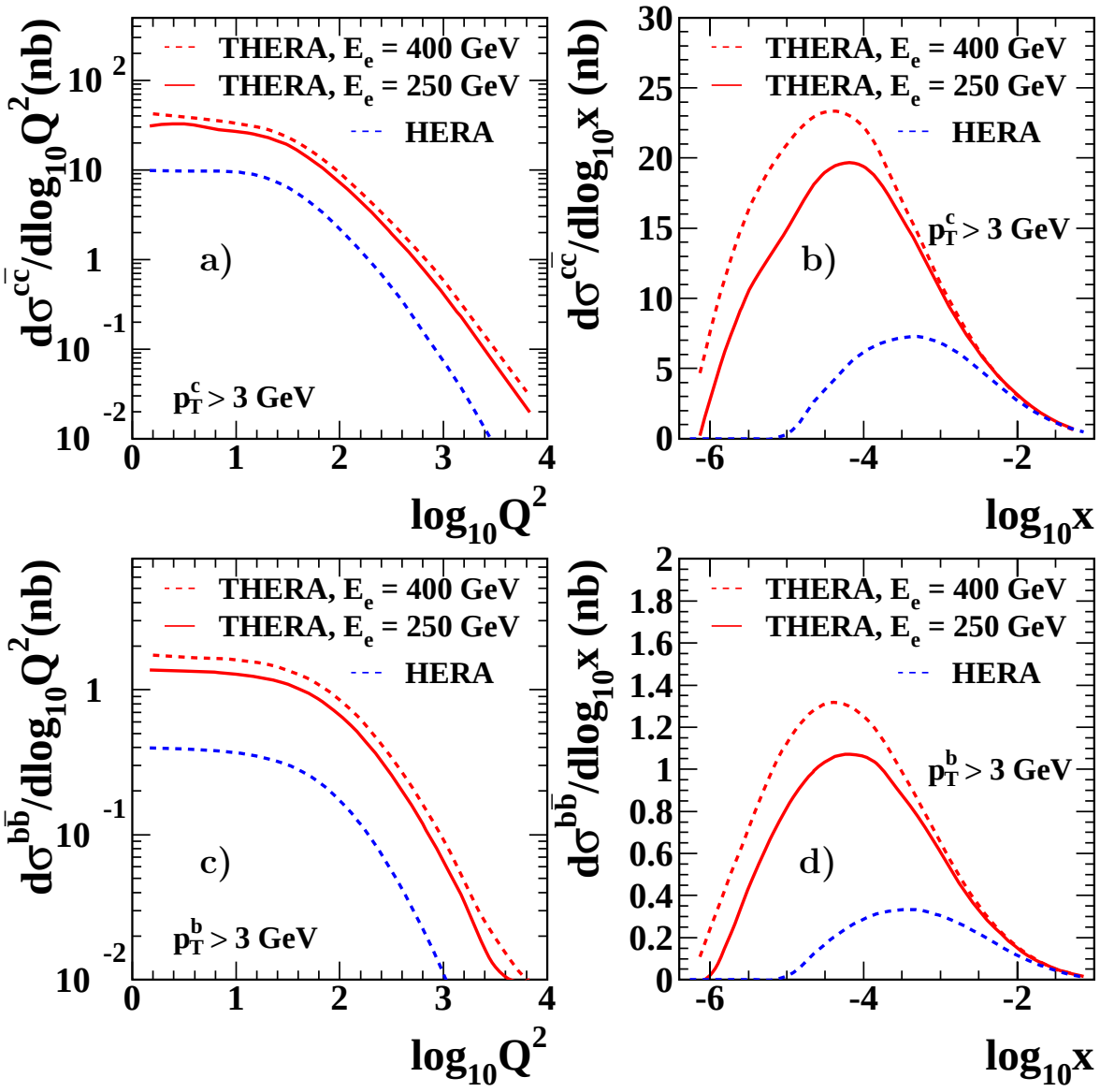

Figure 6: The differential cross sections $d\sigma/d\log_{10}Q^2$ ((a) and (c)) and $d\sigma/d\log_{10}x$ ((b) and (d)) for charm ((a) and (b)) and beauty ((c) and (d)) production at THERA (solid curves) and HERA (lower dashed curves). The upper dashed curves correspond to THERA operation with $E_e = 400\,\mathrm{GeV}$.

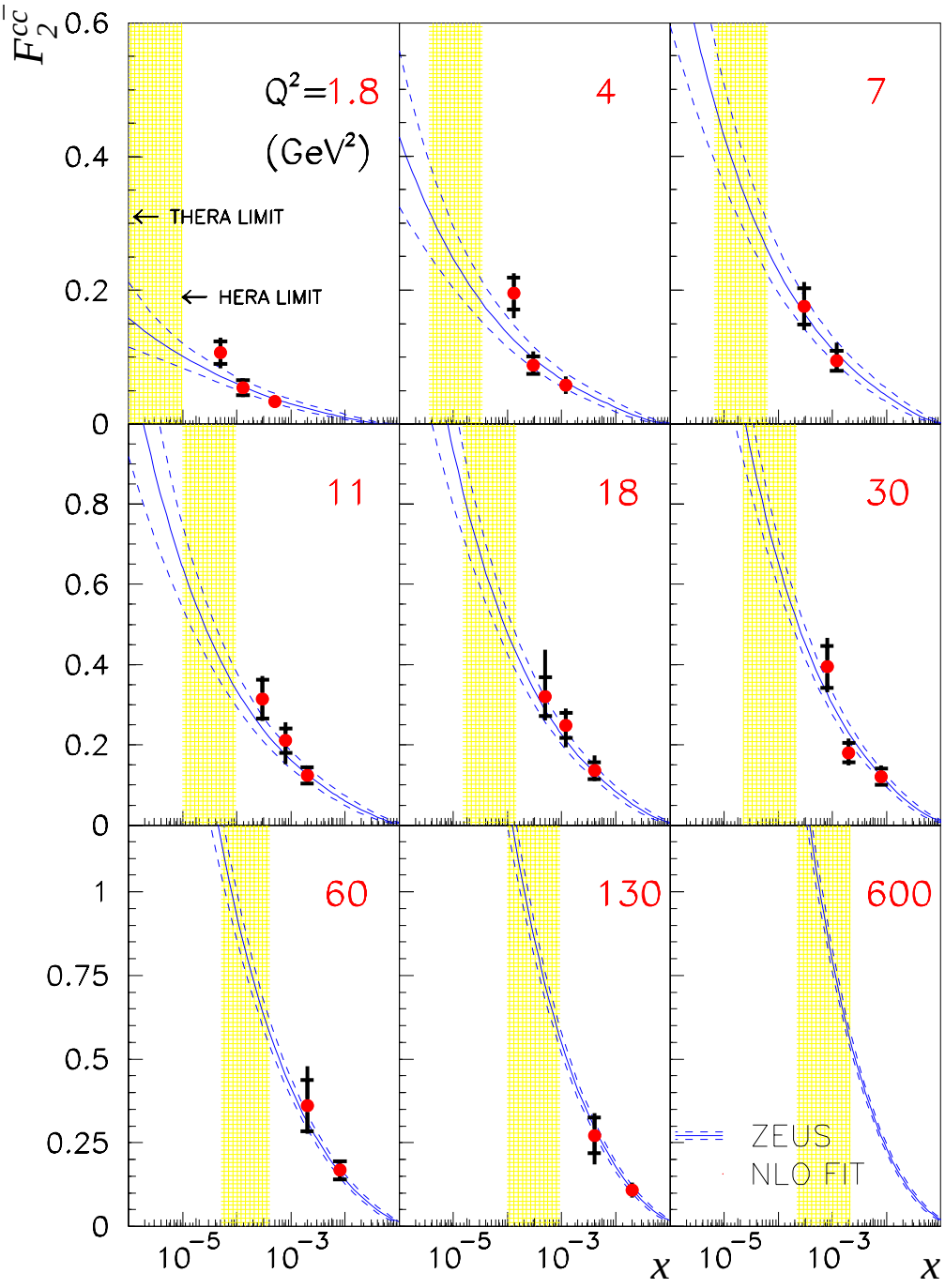

Figure 7: $F_2^{c\bar{c}}$ at Q^2 values between 1.8 and 600 GeV^2 as a function of x. The curves correspond to the three flavour FFNS NLO QCD calculation using the parton distributions from the ZEUS NLO fit. The solid curves correspond to the central values and the dashed curves give the uncertainty due to the parton distributions from the ZEUS NLO fit. The vertical shaded (yellow) bands show the small x extension from HERA to THERA for every Q^2. The $F_2^{c\bar{c}}$ values measured by the ZEUS collaboration are shown as an illustration.

4 Charm production in charged current DIS

The theoretical description of charm production in charged current (CC) DIS is challenging [**?**]. The special interest in this process is caused by its sensitivity to the proton strange-quark density which is rather poorly known [**?**]. However, no measurements of CC charm production have been performed at HERA so far due to the small process cross section ($\sim 10\,\mathrm{pb}$). According to the LO Monte Carlo HERWIG calculation, the cross sections for both LO CC charm production processes, $W^+s \to c$ and $W^+g \to c\bar{s}$, will be more than 6 times larger at THERA than at HERA. The differential cross sections $d\sigma/d\log_{10} Q^2$ and $d\sigma/d\log_{10} x_{s,g}$ ($x_{s,g}$ denoting the parton fractional momenta in the proton) for CC charm production are shown in Fig. 8. The THERA cross sections are shifted towards larger Q^2 with respect to those at HERA. They are one order of magnitude larger than the HERA cross sections at large Q^2 values, thereby creating the opportunity to study charm production in CC DIS at THERA. Fig. 8 shows also that charm production in CC at THERA is sensitive to much wider ranges in $x_{s,g}$ with respect to those at HERA.

The separation of the strange see contribution to the charm production in CC will require a special experimental procedure. It could utilize the different kinematics of $W^+s \to c$ and $W^+g \to c\bar{s}$ processes. Fig. 9 shows the differential cross sections $d\sigma/dp^c_\perp$ and $d\sigma/d\eta^c$ for the processes at HERA and THERA. The pseudorapidity distributions are rather close for both processes while the $p^c_\perp$ distributions are remarkably different. The boson–gluon fusion component is a few orders of magnitude larger than the strange see component at small $p^c_\perp$ values. At large $p^c_\perp$ values both component contributions are similar. Tagging charm quarks with $p^c_\perp$ above a few GeV suppresses effectively the boson–gluon fusion component contribution. Further separation of the strange see contribution will probably require a selection of events with only one jet representing the charm quark.

5 Summary

The total cross sections of charm and beauty production at THERA are expected to increase by factors of three and five, respectively, as compared to HERA. Heavy quarks can be measured at THERA in wide ranges of their transverse momenta, thereby providing a solid basis for testing the pQCD calculations. The gluon structure of the proton can be probed at THERA in as yet unexplored ranges. The kinematic limits of the x_g measurements are 10^{-5} and 10^{-4} for charm and beauty production, respectively. The measurements will require the special tracking and muon identification devices in the backward (electron) direction.

THERA will open new regions for the heavy quark DIS production never measured before. For all Q^2 values the kinematic limit in x at THERA is ~ 1 order of magnitude smaller with respect to that at HERA. Measuring the extreme low x (10^{-5}–10^{-6}) regime is an experimental challenge. If the luminosity turns out to be comparable with final HERA numbers, beauty and charm production at high Q^2 values will benefit from the $3-5$ times larger cross sections at THERA.

The cross section of charm production in charged current at THERA is ~ 1 order of magnitude larger than that at HERA, thereby creating the opportunity to study the process.

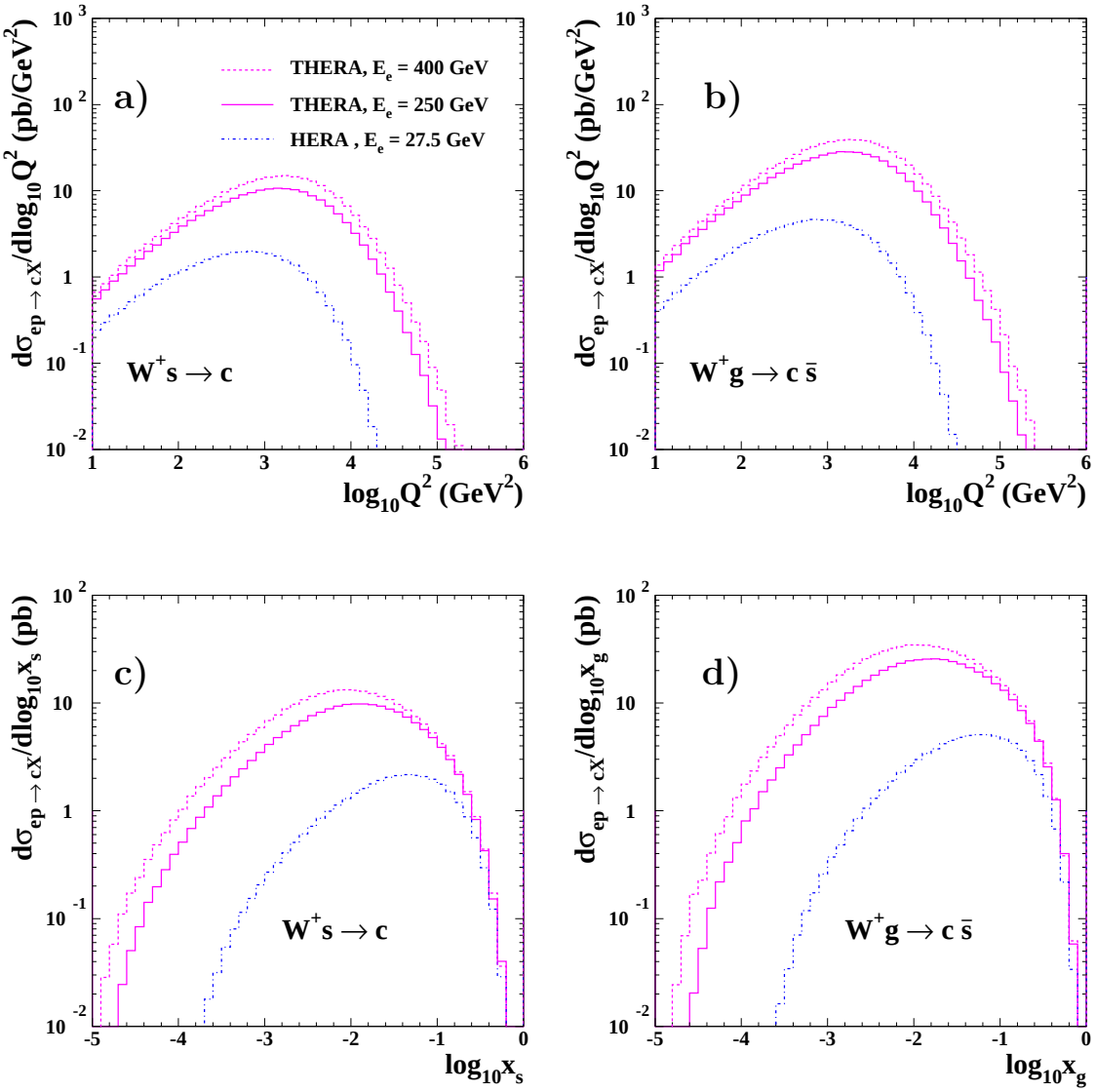

Figure 8: The differential cross sections $d\sigma/d\log_{10}Q^2$ and $d\sigma/d\log_{10}x_{s,g}$ for charm production in charged current DIS from the strange sea ((a) and (c)) and from boson–gluon fusion ((b) and (d)), calculated with the LO Monte Carlo generator HERWIG. The solid and dashed magenta curves show the predictions for THERA operation with an electron energy of 250 GeV and 400 GeV, respectively, and $E_p = 920$ GeV. The predictions for the HERA case are indicated by the dash-dotted blue curves.

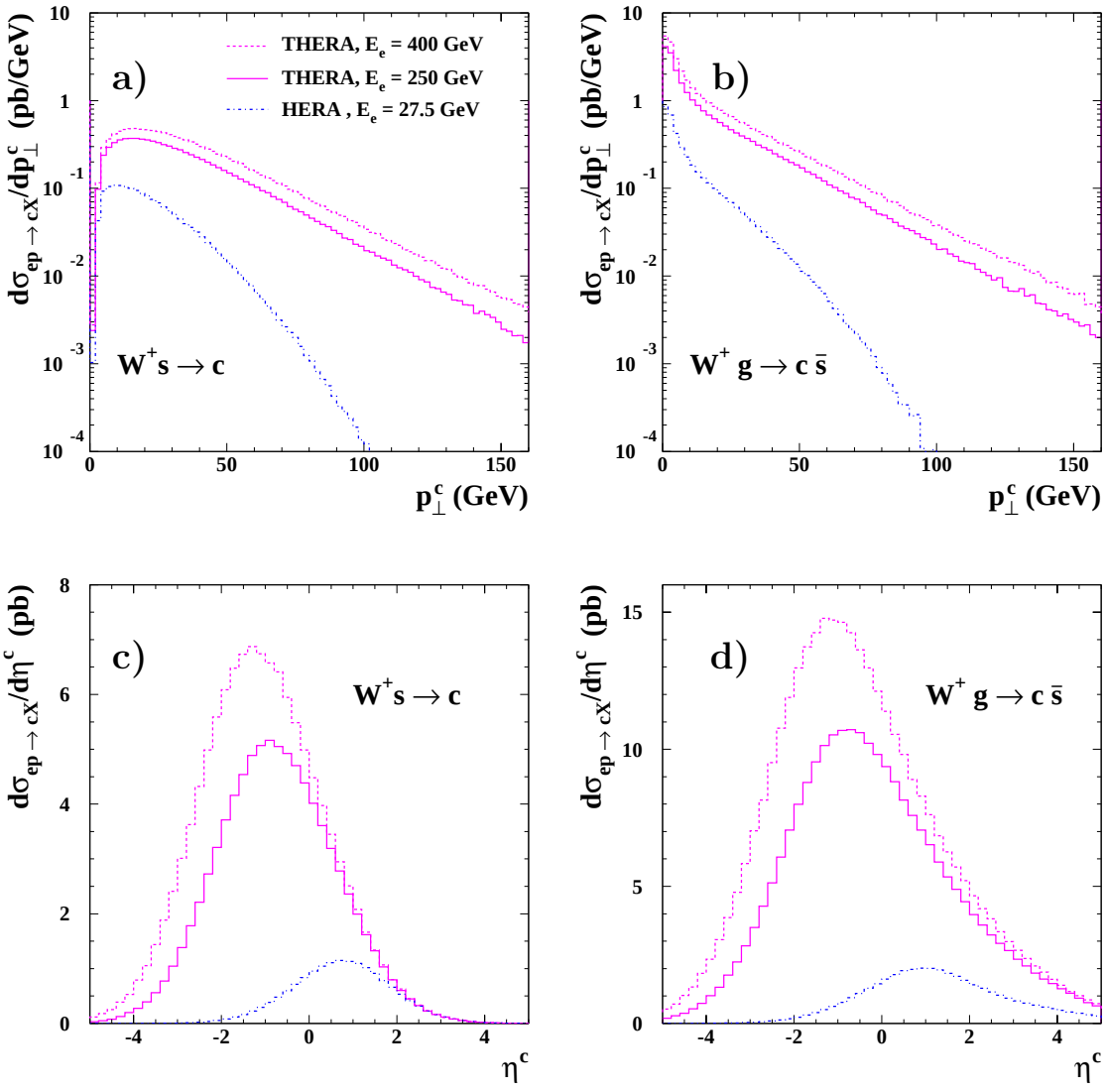

Figure 9: The differential cross sections $d\sigma/dp_\perp^c$ and $d\sigma/d\eta^c$ for charm production in charged current DIS from the strange sea ((a) and (c)) and from boson–gluon fusion ((b) and (d)), calculated with the LO Monte Carlo generator HERWIG. The solid and dashed magenta curves show the predictions for THERA operation with an electron energy of 250 GeV and 400 GeV, respectively, and $E_p = 920$ GeV. The predictions for the HERA case are indicated by the dash-dotted blue curves.

Acknowledgments

We would like to thank S. Frixione and B. Harris for providing us with the programs for their NLO calculations.